

# HIGH-FREQUENCY PLASMA HEATING IN A TOROIDAL TRAP

A.Yu. Voloshko, V.S. Vitsenya, A.V. Longinov, G.A. Miroshnichenko, G.Ya. Nizhnikh, and S.I. Solodovchenko

Physico-technical Institute, Ukrainian Academy of Sciences

Submitted 5 June 1972

ZhETF Pis. Red. 16, No. 2, 80 - 83 (20 July 1972)

Various methods of high-frequency plasma heating in closed magnetic traps have been intensively studied recently [1 - 3], and specific requirements connected with the structural features of the toroidal installations have been formulated for the systems used to excite the high-frequency waves.

We demonstrate in this communication the possibility of effectively introducing HF energy into the plasma by using a system that produces on the plasma periphery a spatially-periodic HF field  $E_z$  parallel to the confining magnetic field. Such a system excites in the plasma mainly slow waves [4], for which  $E_z \gg E_\phi$ . We present here preliminary results on plasma heating in the metallic chamber of the "Saturn" toroidal stellarator-torsatron [5]. When slow waves are excited in a plasma of density  $10^{10} \text{ cm}^{-3}$  in the frequency band  $\omega_h \geq \omega > \omega_{Hi}$  (where  $\omega_h$  and  $\omega_{Hi}$  are the lower hybrid and the ion-cyclotron frequencies), an appreciable heating of the ions and electrons is observed, to energies on the order of 1 keV.

Figure 1 shows a diagram of the setup.

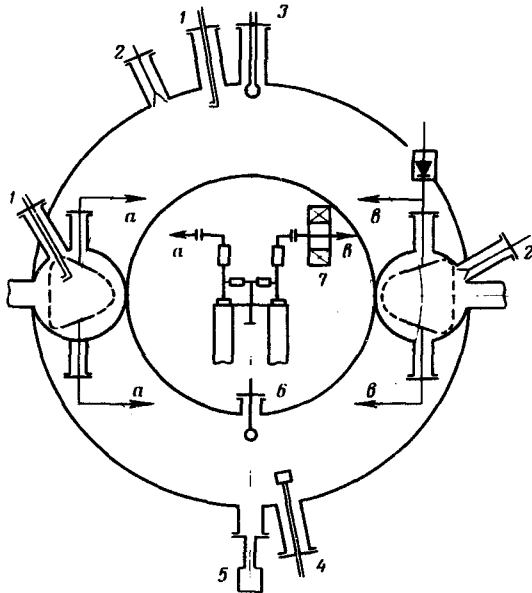


Fig. 1. Diagram of apparatus:  
 1 - probes for the measurement of the HF field  $E_r$ , 2 - 8 mm horns,  
 3 - titanium plasma source,  
 4 - multigridded probe, 5 - photomultiplier, 6 - magnetic probe,  
 7 - Rogowski loop.

The excitation system consisted of four aluminum electrodes, pairwise placed in diametrically opposite sections of the vacuum chamber. The electrode geometry was determined by the construction of the apparatus and was not optimal from the point of view of effective excitation. The shape and position of the electrodes corresponded approximately to the outermost undisturbed magnetic surface (dashed line in Fig. 1). The HF potential of one electrode pair (a) differed by a phase angle  $\pi$  from the potential of the second pair. The operating frequency was 16 MHz. The power input did not exceed 800 W.

The experiments were performed with a residual pressure  $10^{-7}$  Torr in the chamber. The hydrogen plasma was produced by titanium source 3. The HF voltage pulse was applied 400  $\mu\text{sec}$  after the operation of the plasma source, so that all the processes were investigated in the presence of a HF potential on the electrodes. The degree of plasma ionization at the instant of turning on the HF pulse was 20 - 30%.

The plasma density was measured with a double electric probe and by the multimode-resonator method [6]. The

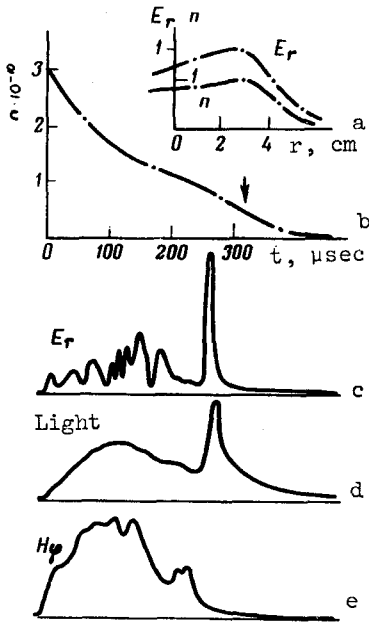


Fig. 2

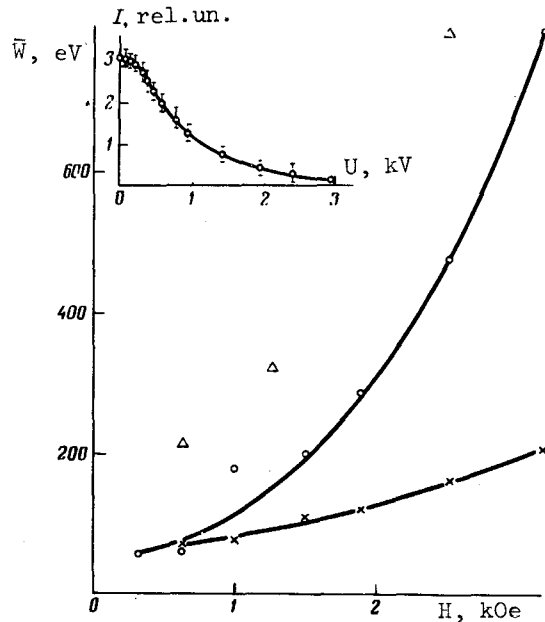


Fig. 3

Fig. 2. a) Radial distribution of HF field  $E_r$  and of the plasma density  $n$ . b - e) Time dependence of the plasma density (b), of the HF field component (c), of the integral plasma glow (d), and of the  $H_\phi$  component (e).

Fig. 3. Charged-particle energies vs. the confining field when the probe is located at  $r = 3.5$  cm. Triangles and crosses -  $W_{e||}$  and  $W_{e\perp}$  respectively at  $\omega_{pi} > \omega$ ; circles -  $W_{i\perp}$  at  $\omega_{pi} = \omega$ ; insert - electron current in collector of multigrad probe vs. the analyzing voltage.

components  $E_r$  and  $H_\phi$  of the HF field in the plasma were registered with electric and magnetic probes (1 and 6). The integral glow of the plasma was registered with photomultiplier 5. The plasma particle energy was measured with multigrad probe 4, using a broadband measuring circuit (up to 35 MHz) which recorded the current to the probe collector. We analyzed the longitudinal electron energy (relative to the magnetic field) and the transverse ion energy.

Figures 2c and 2d show oscillograms of some of the signals, the start of which coincides with the instant when the HF pulse is turned on. The absolute value of the density in Fig. 2b pertains to the central region of the plasma; the arrows mark the density at which  $\omega_{pi} = \omega$ .

It follows from the experimental results that during the HF pulse there exist two different stages of the process: initial, when  $\omega_{pi} \approx \omega_h > \omega$  at the center of the plasma, and final, when  $\omega_{pi} \lesssim \omega$  in the same region (the inequalities  $\omega_{Hi} < \omega_{pi} < \sqrt{\omega_{Hi}\omega_{He}}$  hold true in the investigated magnetic-field range  $H = 300 - 3000$  Oe, so that the plasma ion frequency is comparable with the lower hybrid frequency).

The investigation of the time dependence of the multigrad-probe collector current indicates that an appreciable fraction of the current oscillates at

the frequency of the excited oscillations, which is particularly appreciable when the longitudinal electron energy is analyzed in the second stage of the process. During the initial stage, the amplitude of the ac component of the electron current does not exceed 50% of the dc component. The modulation of the ion current is less than 30% during the entire process. The indicated relations offer evidence that disordered particle motion in the plasma predominates.

A typical plot of the dc component of the electron current to the collector against the analyzing voltage is shown in the insert of Fig. 3. The plots for the ion current are similar. The average energies per particle,  $\overline{W}_{i\perp}$  and  $\overline{W}_{e\parallel}$ , determined from these plots, are shown in Fig. 3.

The time behavior of the components  $E_r$  and  $H_\phi$  of the high-frequency field (Figs. 2c and 2e) and the observed relation between  $\overline{W}_e$  and  $\overline{W}_i$  agree with the possibility of exciting ion-acoustic oscillations with a broad longitudinal wave-number spectrum during the first stage of heating. Such a possibility follows from the theoretical analysis of the electrodynamic characteristics of the employed exciting system. The indicated oscillations are a continuation of the slow-wave branch into the region  $k_{\parallel} > (\omega/v_{Te})$ , and can propagate in the interior when  $\omega < \omega_h$  ( $k_{\perp} \sim \omega/v_s$ , where  $v_s = \sqrt{T_e/m_i}$ , and are damped via Cerenkov absorption by the electrons. The ion heating can be attributed to cyclotron absorption of ion-acoustic oscillations, and also of potential ion-cyclotron waves, which can be excited by the elements directly during the initial stage of the process.

It should be noted that the times of Coulomb relaxation of the distribution function under the conditions of the described experiments greatly exceed the characteristic time of the process. Under these conditions, the observed randomization of the particle coherent motion may be due to nonlinear effects that can result from either the cyclotron or the Cerenkov mechanism.

During the second stage of the process, when the plasma density corresponds to hybrid resonance ( $\omega_h \approx \omega$ ), an appreciable increase of the amplitude of the field  $E_r$  is observed. Figure 2a shows together with the radial distribution of the plasma density (in the absence of an HF pulse) the distribution of the amplitude of the field  $E_r$ . It is seen from Fig. 3 that during this stage the ion heating is the strongest and is apparently due to cyclotron absorption of both the slow electromagnetic wave and of the plasma oscillations with  $k_{\perp}\rho_i > 1$ , which are excited in the transformation region [4, 7].

Our results thus demonstrate the feasibility of heating plasma in a closed magnetic trap by using exciting systems that produce a longitudinal HF electric field in the frequency regions  $\omega < \omega_h$  and  $\omega \approx \omega_h$ .

In conclusion, we are grateful to K.N. Stepanov, V.A. Suprunenko, and V.T. Tolok for useful discussions, and to V.N. Dolya and S.Ya. Slyusarenko for help with the work.

- [1] M.A. Rothman, P.M. Sinclair, I.C. Brown, and J.C. Hosea, *Physics of Fluids* 12, 2211 (1969).
- [2] S.S. Ovchinnikov, S.S. Kalinichenko, O.M. Shvets, and V.T. Tolok, *ZhETF Pis. Red.* 12, 277 (1970) [*JETP Lett.* 12, 187 (1970)].
- [3] V.L. Vdovin et al., *ibid.* 14, 228 (1971) [14, 149 (1971)].
- [4] L.I. Grigor'eva, A.V. Longinov, A.I. Pyatak, V.L. Sizonenko, B.I. Smerdov, K.N. Stepanov, and V.V. Chechkin, Paper IAEA/CN-28/L-7, Madison, Wis., 1971.
- [5] V.S. Voitsenya et al., *Atomnaya Energiya* 31, 536 (1971).

- [6] D.A. Akulina and Yu.I. Nechaev, *Teplofiz. Vys. Temp.* 6, 1061 (1969).  
 [7] T.H. Stix, *Phys. Rev. Lett.* 15, 878 (1965).

SPIN-LATTICE RELAXATION IN CRYSTALS WITH SOFT OPTICAL PHONONS

D.E. Khmel'nitskii and V.L. Shneerson  
 L.D. Landau Institute of Theoretical Physics  
 Submitted 4 July 1972  
 ZhETF Pis. Red. 16, No. 2, 84 - 85 (20 July 1972)

As is well known, the spin-lattice relaxation is due to phonon-scattering processes that are accompanied by spin flip. The probability of such processes is proportional to the phonon occupation numbers and also to the relative displacement of the lattice atoms. At low temperatures the main contribution is usually made by the long-wave acoustic oscillations. For such oscillations, the relative displacements of the nearest neighbors are small. The relaxation time is proportional to  $(\theta/T)^7$  [1].

In some substances (SnTe, SrTiO<sub>3</sub>, and KTaO<sub>3</sub>) the oscillation spectrum has a low-lying optical branch for which  $\omega^2(k) = \omega_0^2 + sk^2$ . At temperatures  $\omega_0 \lesssim T \ll \theta$ , the number of thermal optical phonons is of the order of the number of acoustic ones, and the relative displacements of the nearest neighbors are not small even in the case of long waves. Therefore the scattering of the optical phonons will be the principal mechanism of spin relaxation, and the relaxation probability will be proportional to a lower power of the temperature.

The spin-phonon Hamiltonian can be written in the form

$$H_{sp} = \sum_{\vec{l}, \vec{l}'} \hat{C}_i^{\alpha\beta}(\vec{l}, i, \vec{l}', i') v_i^\alpha(\vec{l}, i) v_i^\beta(\vec{l}', i'), \quad (1)$$

where

$$\hat{C}_i^{\alpha\beta}(\vec{l}, i, \vec{l}', i') = \frac{1}{6} \hat{Q}_{\mu\nu} \frac{\partial^4 V}{\partial R_i^\mu \partial R_i^\nu \partial R_{i'}^\alpha \partial R_{i'}^\beta}$$

We have in mind here the quadrupole relaxation mechanism, which is realized for spins  $j \geq 1$ .  $\hat{Q}_{\mu\nu}$  is the operator of the quadrupole moment that interacts with the gradients of the crystal potential  $V$ .  $\vec{v}_1(\vec{l}, j) = \vec{u}(\vec{l}, j) - \vec{u}(0, i)$  is the vector of the relative displacement of the atoms type  $j$  in the cell  $\vec{l}$  and of the atom of type  $i$ , which carries the spin, in the cell 0. In the case of ionic crystals  $\hat{C}(\vec{l}, j, \vec{l}', j') = \hat{C}(\vec{l}, j) \delta_{\vec{l}\vec{l}'} \delta_{ii'}$ .

Using the Hamiltonian (1) we can calculate the probability of the transition between states with spin projections  $m$  and  $m'$ . It must be taken into account here that the Zeeman energy is low ( $\epsilon_m - \epsilon_{m'} \ll T$ ). We obtain finally

$$W_{mm'} = \frac{2}{27\pi} \frac{v_0}{\mu^2 s^3} T^3 \sum_{\vec{l}, i, i'} \langle m' | C_i^{\alpha\beta}(\vec{l}, i) | m \rangle \times \langle m | C_i^{\alpha\beta}(\vec{l}', i) | m' \rangle \quad (2)$$

For concreteness, the crystal was assumed to be diatomic and cubic ( $\mu$  is the reduced mass and  $v_0$  is the volume of the cell), while the soft branch was